Spectrochimica Acta Part A: Molecular and Biomolecular Spectroscopy 179 (2017) 221–226

Contents lists available at ScienceDirect

Spectrochimica Acta Part A: Molecular and Biomolecular Spectroscopy

journal homepage: www.elsevier.com/locate/saa

A highly selective and sensitive rhodamine-derived fluorescent probe for detection of Cu^{2+}

Linlin Lv, Quanping Diao *

School of Chemistry and Life Science, Anshan Normal University, Ping'an Street 43, Anshan 114005, China

ARTICLE INFO

Article history:
Received 23 December 2016
Received in revised form 14 February 2017
Accepted 22 February 2017
Available online 24 February 2017

Keywords:
Fluorescence
Probe
Rhodamine
Cu^{2+}
DFT
Living cells
Drinking water

ABSTRACT

A novel water-soluble and reversible fluorescent probe was designed and synthesized based on a rhodamine B derivative. It was used for detection of Cu^{2+} in drinking water and in living cells with high sensitivity and excellent selectivity. The tested concentration range and the limit of detection (LOD) of the probe were 0–15.00 μmol L^{-1} and 0.085 μmol L^{-1}, respectively. In addition, the mode of binding and mechanism of interaction between the probe and Cu^{2+} were analyzed by density functional theory (DFT) calculations.

1. Introduction

As a soft transition metal that plays pivotal roles in various physiological processes, the content of copper (Cu) is lower than that of iron and zinc in the body [1]. However, excessive accumulation of Cu leads to severe toxicity [2,3]. For example, short-term exposure to an environment with high concentration of Cu^{2+} causes gastrointestinal discomfort in the human body, while a long-term exposure can lead to liver and kidney damage [4]. Therefore, the World Health Organization (WHO) and the United States Environmental Protection Agency (EPA) have set the maximum allowable level (MAL) of Cu^{2+} in drinking water at 2.0 mg L^{-1} and 1.3 mg L^{-1}, respectively [5]. Currently, the methods for detection of Cu^{2+} mainly include [6–8](AAS), atomic emission spectrometry (AES) [9,10], atomic fluorescence spectrometry (AFS) [11], and inductively coupled plasma–mass spectrometry (ICP–MS) [12,13], and so on. However, these methods require expensive equipment and complicated sample preparation procedures, and therefore, cannot be used for detection of Cu^{2+} in living tissues. Hence, it is important to develop a simple method for rapid estimation of Cu^{2+} concentration in drinking water and in the human body.

Currently, fluorescent probe sensing is one of the most rapid and developed detection methods for metal ions [14–24]. Compared to the traditional detection methods, it shows several significant advantages such as low cost, ease of operation, high sensitivity, and fast response [25–28]. In addition, the development of novel fluorescent probes has also boosted the development of diagnostic techniques for imaging live biomedical and medical samples [29–32]. Among the various known fluorescent dyes, rhodamine and its derivatives received great attention owing to their excellent photo-physical properties such as high fluorescence quantum yield, excitability by visible light, relatively long emission wavelength, and superior photo-stability [33,34]. Generally, the molecular structure of rhodamine derivatives can be changed from the spiro-ring to the open-ring forms by altering the chemical environment, and hence these molecules exhibit distinct fluorescence properties.

As early as 1997, Czarnik et al. designed and synthesized the first fluorescent probe with a rhodamine B hydrazide structure for detection of Cu^{2+} [35]. It was found that the formation of coordination complexes between rhodamine hydrazide and Cu^{2+} led to the ring opening of spirolactam, which could be further hydrolyzed to produce a strong fluorescent emission spectrum in a neutral HEPES buffer solution accompanied by color change of the solution. Later in 2006, Toon et al. introduced a salicylaldehyde group based on the structure of rhodamine hydrazide to synthesize the fluorescent probe salicylaldehyde rhodamine B hydrazine for the detection of Cu^{2+} [36]. This probe greatly enhanced the ability of the system to complex with Cu^{2+}, with a complexation constant above 10^6 L mol^{-1}. The lowest detection limit of Cu^{2+} achieved micromolar levels in acetonitrile and Tris-HCl buffered solution (pH = 7.0) without the interference of other ions. Thereafter, studies on the design and synthesis of Cu^{2+}-selective fluorescent probes utilizing rhodamine derivatives has received increased attention of scientific researchers. Recently, researchers have developed better

* Corresponding author.
E-mail address: quanpingdiao@163.com (Q. Diao).

http://dx.doi.org/10.1016/j.saa.2017.02.053
1386-1425/

recognition sites by changing the structure of the probe, continuously improved the sensitivity and selectivity of the probe, and expanded its applications [37–48]. In this study, we designed and synthesized a novel fluorescent probe (RBA) based on rhodamine B and 3-formyl-2-hydroxybenzoic acid for detection of Cu^{2+}. Compared with the reported probe, the probe RBA presented in this work provides better selectivity and sensitivity, and was further applied for practical samples such as drinking water and living cells.

2. Experimental Details

2.1. Chemicals and Reagents

Rhodamine B (96%) and salicylic acid (99%) were purchased from J&K Chemical Ltd. Salts of all the cations, that is, $Cu(ClO_4)_2 \cdot H_2O$, $Mg(ClO_4)_2 \cdot 6H_2O$, $Zn(ClO_4)_2 \cdot 6H_2O$, $Co(ClO_4)_2 \cdot 6H_2O$, $Cd(ClO_4)_2 \cdot H_2O$, $Ni(ClO_4)_2 \cdot 6H_2O$, $Mn(ClO_4)_2 \cdot 6H_2O$, $Ba(ClO_4)_2 \cdot 6H_2O$, $Ca(ClO_4)_2 \cdot 6H_2O$, $Fe(ClO_4)_3 \cdot 6H_2O$, and $Hg(ClO_4)_2 \cdot xH_2O$ were purchased from Energy Chemical Reagent Co., Ltd. Other reagents used here were analytical reagent grade and used without further purification or treatment. All aqueous solution was prepared with ultrapure water with Milli-Q water purification system (18.2 MΩ cm).

2.2. Instruments

UV–Vis and fluorescence spectra were recorded on a Cary 60 spectrophotometer (Agilent Technologies, USA) and a Cary Eclipse spectrofluorophotometer (Agilent Technologies, USA), respectively. Spectra of ^{1}H NMR (TMS as internal standard) were measured on a Mercury 300BB nuclear magnetic resonance spectrometer (Varian Inc., USA). MS spectra were obtained by a LC/MS QTRAP spectrometer (SCIEX Inc., USA). All pH measurements were made with a PHS-3C pH-Meter (INESA Scientific Inc., China). Living cells were imaged by an Olympus IX 71 inverted fluorescence microscopy (Olympus Corporation, Japan) equipped with integrated color filters, using green light excitation (510–550 nm).

2.3. Synthesis of Probe RBA

The synthetic route of RBA is shown in Fig. 1.

2.3.1. Synthesis of Compound **1**

Compound **1** was synthesized from salicylic acid according to the reported method [49]. 1.38 g of salicylic acid (10 mmol) and about 6.0 mL of ethanol were put into a 100 mL bottom flask. Then 15 mL of 50% NaOH solution, 3.0 mL of $CHCl_3$ (40 mmol), and 50 mg of dibenzo-18-crown-6 (catalytic amount) were added in the flask. The reaction temperature was maintained at 55 °C and the mixture was stirred for 24 h. Having been cooled, the mixture was acidified with 10 mol L^{-1} H_2SO_4. The crude product was recrystallized from ethanol. Finally, 0.48 g of compound **1** as a white solid (yield 29%) was obtained. ^{1}H NMR (300 MHz, d^6-DMSO) δ 9.88 (s, 1H), 8.35 (d, 1H), 8.00 (m, 1H), 7.12 (d, 1H).

2.3.2. Synthesis of Compound **2**

Compound **2** was synthesized from Rhodamine B according to the reported method [36]. 1.2 g of Rhodamine B (2.5 mmol) and 50 mL of ethanol were placed into a 100 mL bottom flask. Then 4.0 mL of hydrazine hydrate (excess) was added into the flask. The mixture was refluxed for 6 h till the color of the solution was changed from dark purple to light orange. Then the mixture was cooled and the solvents were removed under reduced pressure. 60 mL of 1 mol L^{-1} HCl was added to the flask to generate a clear red solution. After that, 1 mol L^{-1} NaOH was added slowly with stirring until the pH of the solution reached 9. The precipitate produced was filtered and washed 3 times with water, and dried over P_2O_5 under vacuum. The 0.78 g of compound **2** as pink solid (yield 68%) was obtained. ^{1}H NMR (300 MHz, d^6-DMSO) δ 7.87–7.66 (m, 1H), 7.56–7.39 (m, 2H), 7.07–6.91 (m, 1H), 6.36 (d, 6H), 3.32 (dd, 8H), 1.08 (t, 12H).

2.3.3. Synthesis of Compound RBA

0.17 g of compound **1** (1 mmol) was added in 25 mL of absolute ethanol containing 0.46 g of compound **2** (1 mmol). The resulting mixture was refluxed and stirred for 24 h. The solvent was removed under reduced pressure to give a purple solid. The crude product was purified by chromatography on silica gel using CH_2Cl_2:methanol (10:1, v/v) as an eluent. The 0.46 mg of RBA as purple solid (yield 76%) was obtained. ESI-MS: m/z 605.3 for $[RBA + H]^+$. ^{1}H NMR (300 MHz, $CDCl_3$) δ 8.56 (s, 1H), 8.06 (dd, 1H), 7.60–7.44 (m, 2H), 7.27–7.08 (m, 2H), 6.73 (dd, 4H), 6.41 (s, 2H), 3.35 (dd, 8H), 1.17 (t, 12H).

2.4. Spectrophotometric Experiments

The probe RBA was dissolved in DMF to get a 1 mmol L^{-1} standard solution. 20 μL of this standard solution was added into 2 mL CH_3CN/H_2O mixture (3:7, v/v; HEPES buffer 50 mmol L^{-1}; pH = 7.4) containing testing cations and allowed to stand for 15 min at room temperature before fluorescence and UV–Vis measurements. Blank solution of RBA without cations was prepared by the same procedure. The fluorescence emission spectra were excitation wavelength at 535 nm. Both the excitation and emission slits were set at 5.0 nm.

2.5. Preparation of Cells

The HeLa Cells were grown in Dulbecco's modified Eagle's medium (DMEM) supplemented with 10% fetal bovine serum and 1% penicillin–streptomycin, incubated under a humidified atmosphere of 5% CO_2 and 95% air at 37 °C for 24 h. Cells were seeded on dish for fluorescence microscopic imaging by inversion fluorescence microscope.

3. Results and Discussion

3.1. Fluorescence and Absorbance Spectra

The fluorescence emission spectrum of RBA in CH_3CN/H_2O mixture (3:7, v/v; HEPES buffer 50 mmol L^{-1}; pH = 7.4) solution is shown in Fig. 2. RBA showed very weak fluorescence emission with a low

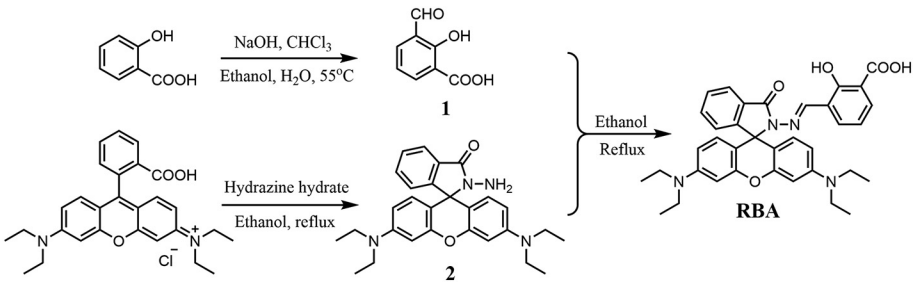

Fig. 1. Synthetic route of probe RBA.

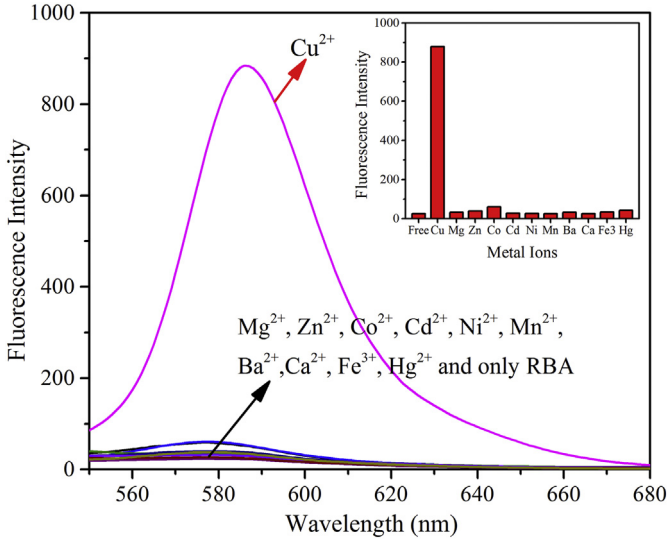

Fig. 2. Fluorescence emission spectra of RBA (10 mol L^{-1}) in CH_3CN/H_2O mixture (3:7, *v/v*; HEPES buffer 50 mmol L^{-1}; pH = 7.4) solution, in the absence and presence of common metal ions (2×10^{-4} mol L^{-1}). Excitation wavelength was 535 nm.

absolute quantum yield ($\Phi = 0.04$) under the excitation wavelength of 535 nm. This was due to the spirolactam ring form of its molecular structure, and RBA did not show the typical emission peak of the rhodamine skeleton in the wavelength range of 400–600 nm. The influence of metal ions on the fluorescence intensity of the probe was tested by using 11 common metal ions, including Cu^{2+}, Mg^{2+}, Zn^{2+}, Co^{2+}, Cd^{2+}, Ni^{2+}, Mn^{2+}, Ba^{2+}, Ca^{2+}, Fe^{2+}, and Hg^{2+} at the concentration of 2×10^{-4} mol L^{-1}. As shown in Fig. 2, only Cu^{2+} significantly enhanced the fluorescence emission intensity of the RBA probe at 586 nm, with an absolute quantum yield of 0.35. This was because the ring-opening of spirolactam within the RBA molecular structure was induced by the coordination of RBA and Cu^{2+}. This result showed that RBA was suitable for selective detection of Cu^{2+} in the presence of various other ions. Fig. S4 shows that the fluorescence emission intensity of RBA increased with an increase in Cu^{2+} concentration (0–150 μmol L^{-1}).

The UV–visible absorption spectra of RBA in CH_3CN/H_2O mixture (3:7, v/v; HEPES buffer 50 mmol L^{-1}; pH = 7.4) were also studied. As

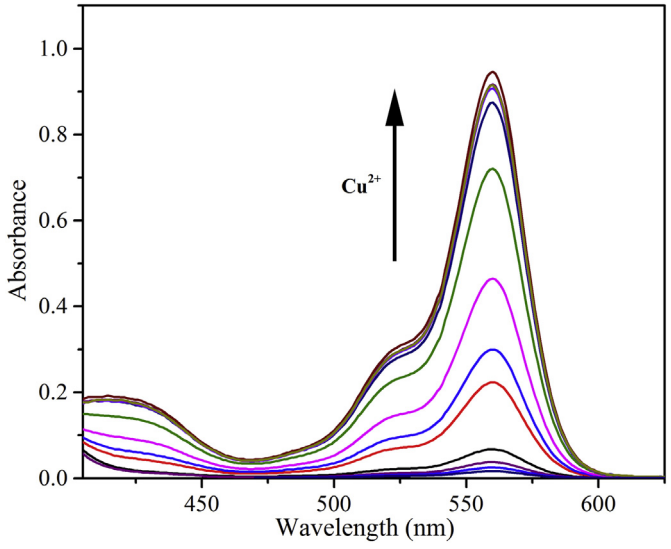

Fig. 3. Absorption spectra of RBA (10 mol L^{-1}) in CH_3CN/H_2O mixture (3:7, v/v; HEPES buffer 50 mmol L^{-1}; pH = 7.4) solution with different concentration levels of Cu^{2+} (0–150 mol L^{-1}).

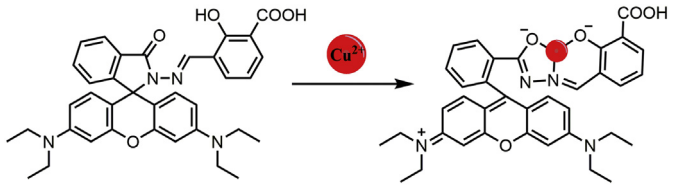

Fig. 4. Predicted spirolactam ring-opening mechanism of RBA induced by Cu^{2+}.

shown in Fig. 3, the color of the solution changed from colorless to strong pink with the addition of Cu^{2+} (150 μmol L^{-1}). The reason for this phenomenon is the same as that for the increase in the fluorescence emission intensity discussed above. The typical absorption peak of rhodamine at 560 nm appeared, and the intensity increased with Cu^{2+} concentration. Therefore, RBA can also be used as a colorimetric probe for selective detection of Cu^{2+}.

3.2. Binding Affinity of RBA to Cu^{2+}

Job's point experiment was used to determine the stoichiometry of coordination between RBA and Cu^{2+}. As shown in Fig. S5, the intersection point of the fluorescence intensities was observed at the molar fraction of ~0.50, indicating that the coordination ratio between RBA and Cu^{2+} was 1:1. Furthermore, ESI-MS showed that the binding ratio of RBA to Cu^{2+} was also 1:1. The ESI-MS spectrum of RBA revealed a main peak at *m/z* 605.3 corresponding to $[RBA + H]^+$. After the addition of 50 μmol L^{-1} of Cu^{2+}, a main peak at *m/z* 666.2 appeared, coinciding exactly with the species of $[RBA + Cu - 2H]^+$ that confirming the 1:1 formation of the RBA-Cu^{2+} coordination. Fig. 4 shows that the predicted mechanism of the spirolactam ring-opening of rhodamine is induced by the coordination of RBA and Cu^{2+}.

To better understand of the coordination chemistry between Cu^{2+} and RBA, the optimized energy structures of the RBA and RBA-Cu complexes (Fig. 5) were obtained using density functional theory (DFT) calculation at the B3LYP level using 6–31G(d,p) basis set for simple receptor (RBA) and LANL2DZ basis set for metal complex with the Gaussian 09 program [50]. The spatial distribution of the electron cloud and the orbital energy of the highest occupied molecular orbital (HOMO) and the lowest unoccupied molecular orbital (LUMO) of RBA and the complex were also calculated. As shown in Fig. 5, the HOMO

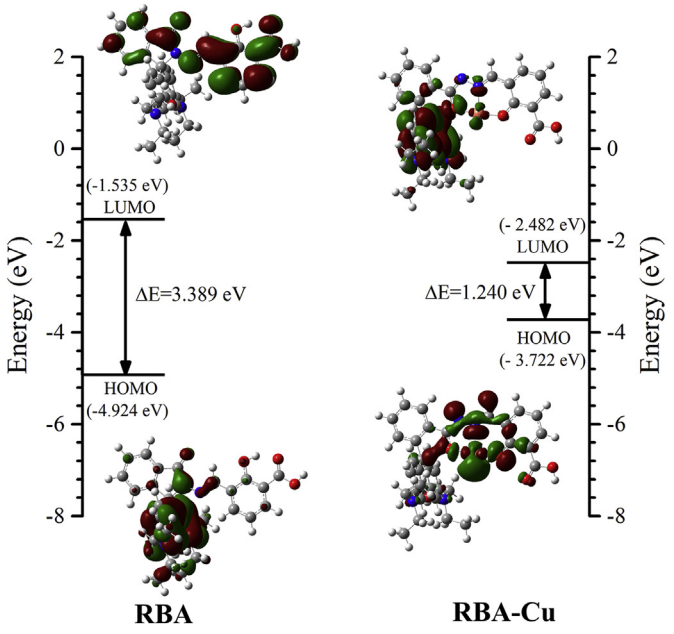

Fig. 5. Energy diagram of HOMO and LUMO orbitals RBA and RBA–Cu complex.

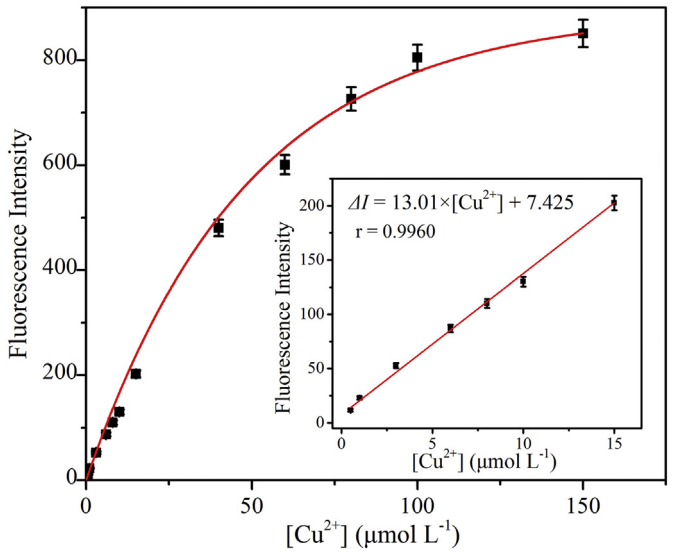

Fig. 6. Curves of the fluorescence intensity at 586 nm versus the concentrations of Cu^{2+}. Inset: calibrations curve in the concentration range of 0 to 15.00 μmol L^{-1} of Cu^{2+}.

of RBA was distributed only at the substituted spirolactam ring, while the LUMO was distributed throughout the molecule. The result showed that when the C—N bond of the spirolactam ring was broken, it could promote the coordination between the ionophore carbonyl oxygen and the metal ion. The π-electrons in the HOMO of RBA-Cu complex were distributed around the metal ion, while that in the LUMO were distributed only in the xanthene moiety. The calculated energy gap (ΔE) between HOMO and LUMO of RBA and RBA-Cu were 3.389 eV and 1.240 eV, respectively, which indicated that the coordination of Cu^{2+} and RBA decreased the energy gap of HOMO-LUMO and stabilized the system. Therefore, an optimal ideal coordination structure was proposed according to the coordination features presented above.

3.3. Influences of Time and pH

The effect of reaction time on the fluorescence intensity of the RBA-Cu complexes was studied at room temperature. Fig. S6 showed that in the presence of Cu^{2+} in CH_3CN/H_2O mixture (3:7, v/v; HEPES buffer 50 mmol L^{-1}; pH = 7.4) solution the fluorescence intensity of RBA increased significantly within 5 min, reached a maximum after 15 min and tended to be stable. This indicated that the coordination of RBA and Cu^{2+} can be completed within 15 min. Therefore, a reaction time of 15 min was applied in the subsequent experiments.

The effect of pH on the fluorescence intensity of the RBA-Cu complex was also investigated under various pH conditions. As shown in Fig. S7, the fluorescence intensity of RBA increased rapidly with a decrease of pH from 6 to 4, indicating that the spirolactam ring of RBA can be opened in acidic solutions. At pH of 6–8, RBA exhibited a highly selective fluorescence "turn-on" response to Cu^{2+}. The pH range of drinking water and living cells is usually between 6.0 and 7.6, therefore the fluorescent probe RBA can be utilized for Cu^{2+} detection in drinking water and living cells.

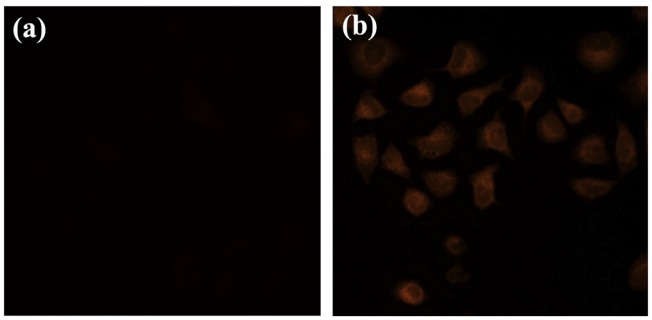

Fig. 7. Fluorescence images of HeLa cells: (a) cells incubated with RBA (10 μmol L^{-1}) for 30 min; (b) cells incubated with Cu^{2+} (10 μmol L^{-1}) for μmol L^{-1} 30 min.

3.4. Reversibility of the Binding of RBA to Cu^{2+}

Reversibility of target ion binding is an important feature of fluorescent probes. Therefore, the chemical reversibility of the binding between RBA and Cu^{2+} was also investigated. It could be seen with the naked eye that the pink color of the RBA-Cu solution disappeared rapidly upon the addition of excess sodium salt of EDTA, and simultaneously, the fluorescence intensity returned to its original level (Fig. S8). These phenomena indicated that the coordination of EDTA-Cu could lead to the dissociation of the RBA-Cu complex, and hence the coordination between RBA and Cu^{2+} was chemically reversible.

3.5. Determination of Cu^{2+}

The standard curve for Cu^{2+} determination was obtained by plotting the fluorescence emission intensity at 583 nm versus the Cu^{2+} concentration (Fig. 6). The calibration curve showed a linear fit in the concentration range of 0–15.00 μmol L^{-1}, with a correlation coefficient (r) of 0.9960. The detection limit of Cu^{2+} concentration was 0.085 μmol L^{-1} (S/N = 3), which is much lower than what has been previously reported [51–55] and most importantly, it falls beneath the MAL of Cu^{2+} in drinking water according to USEPA and WHO regulations. The RBA probe was successfully applied for Cu^{2+} detection in drinking water samples; however, the results showed no significant differences with those obtained by atomic absorption spectroscopy (AAS) (Table 1). Nonetheless, the method for Cu^{2+} detection in drinking water reported here has the advantages of low cost and easy operation compared to AAS.

3.6. Fluorescence Imaging for Living Cells

In order to examine the practical application of RBA in biological research, cytotoxicity and fluorescence imaging experiments were performed in living cells. The toxicity of RBA on HeLa cells was evaluated by the MTT assay in a concentration range of 0 to 20 μmol L^{-1} of RBA (Fig. S9). The results showed that more than 90% of the cells were viable after the incubation, indicating that RBA was non-toxic to the cells under our experimental conditions. Next, the HeLa cells were incubated in phosphate buffer solution containing 10 μmol L^{-1} RBA for 30 min at 37 °C and processed for fluorescence imaging. As shown in Fig. 7a, no fluorescence emission was observed. The cells were then incubated in a medium containing 10 μmol L^{-1} of Cu^{2+} for further 30 min at 37 °C

Table 1
Analytical results of Cu^{2+} in drinking water samples (n = 5).

Sample No.	Spiked (μmol L^{-1})	AAS method			Fluorescent method		
		Found (μmol L^{-1})	RSD (%)	Recovery (%)	Found (μmol L^{-1})	RSD (%)	Recovery (%)
1	10.00	9.92	5.3	99.2	10.08	6.5	100.8
2	10.00	9.77	4.7	97.7	10.11	5.8	101.1

and washed thrice with phosphate buffer solution. This time, fluorescence emission was observed within the cells, as shown in Fig. 7b. These results indicated that the RBA probe can penetrate the cell membrane and can therefore be used for Cu^{2+}-based imaging investigations in living cells.

4. Conclusions

In this work, a novel "turn-on" fluorescent probe based on the spirolactam ring-opening reaction of rhodamine derivatives was developed, which can be used for the detection of Cu^{2+} in drinking water and fluorescence imaging in living cells. The high selectivity of the probe was demonstrated by comparing the characteristics of the fluorescence spectrum in the presence of Cu^{2+} and 10 other metal ions. Analysis of drinking water samples showed that this probe is suitable for the detection of Cu^{2+} in neutral water with high sensitivity and reproducibility. In addition, the probe also showed the potential for monitoring Cu^{2+} in living cells.

Acknowledgements

This work was supported by Program for High-end Talent Training in AnShan Science and Technology Bureau (Nos. 20153473 and 20153499).

Appendix A. Supplementary data

Supplementary data to this article can be found online at http://dx.doi.org/10.1016/j.saa.2017.02.053.

References

[1] M. Valko, C.J. Rhodes, J. Moncol, M. Izakovic, M. Mazur, Free radicals, metals and antioxidants in oxidative stress-induced cancer, Chem. Biol. Interact. 160 (2006) 1–40.
[2] S.J. Stohs, D. Bagchi, Oxidative mechanisms in the toxicity of metal ions, Free Radic. Biol. Med. 18 (1995) 321–336.
[3] M. Valko, H. Morris, M.T.D. Cronin, Metals, toxicity and oxidative stress, Curr. Med. Chem. 12 (2005) 1161–1208.
[4] J.S. Valentine, P.A. Doucette, S.Z. Potter, Copper-Zinc Superoxide Dismutase and Amyotrophic Lateral Sclerosis, Annual Review of Biochemistry, Annual Reviews, Palo Alto, 2005 563–593.
[5] B. Zhang, Q. Diao, P. Ma, X. Liu, D. Song, X. Wang, A sensitive fluorescent probe for Cu^{2+} based on rhodamine B derivatives and its application to drinking water examination and living cells imaging, Sensors Actuators B Chem. 225 (2016) 579–585.
[6] A. Asfaw, G. Wibetoe, Direct analysis of beer by ICP-AES: a very simple method for the determination of Cu, Mn and Fe, Microchim. Acta 152 (2005) 61–68.
[7] E.J. Daftsis, G.A. Zachariadis, Analytical performance of a multi-element ICP-AES method for Cd, Co, Cr, Cu, Mn, Ni and Pb determination in blood fraction samples, Microchim. Acta 160 (2008) 405–411.
[8] M. Yaman, I.H. Yaman, Determination of trace metal levels of Cd, Pb, Cr, Ni, and Cu in Two Fish Species by STAT-MS and ICP-AES, At. Spectrosc. 34 (2013) 191–198.
[9] G.F.B. Cruz, R.J. Cassella, An ionic liquid-based microextraction method for the determination of Cu and Ni in high-salinity produced water from offshore petroleum exploration by GF AAS, Anal. Methods 7 (2015) 6848–6855.
[10] A.M. Hernandez-Martinez, C. Padron-Sanz, M.E. Torres-Padron, Z. Sosa-Ferrera, J.J. Santana-Rodriguez, Analysis of Ni, Cr, Cu, Pb and Cd in marine bioindicators using mixed-micelles with microwave assisted micellar extraction and GF-AAS, Anal. Methods 8 (2016) 7141–7149.
[11] J.P. Fitts, T.P. Trainor, D. Grolimund, J.R. Bargar, G.A. Parks, G.E. Brown, Grazing-incidence XAFS investigations of Cu(II) sorption products at alpha-Al(2)O(3)-water and alpha-SiO(2)-water interfaces, J. Synchrotron Radiat. 6 (1999) 627–629.
[12] S.F. Ferrarini, H.S. dos Santos, L.G. Miranda, C.M.N. Azevedo, S.M. Maia, E.S. Chaves, M.J.R. Pires, Determination of As, Cr, and Cu concentrations in CCA-treated wood poles using acid decomposition in closed flasks, oven heating, and ICP-MS analysis, At. Spectrosc. 36 (2015) 187–195.
[13] R. Yang, Y. Ning, A. Zhang, Y. Li, H. Su, Analysis of Cu, Co, V and Zn in coastal waters of the East China Sea by inductively coupled plasma mass spectrometry (ICP-MS), J. Ocean Univ. China 15 (2016) 825–834.
[14] X. Chen, Y. Zhou, X. Peng, J. Yoon, Fluorescent and colorimetric probes for detection of thiols, Chem. Soc. Rev. 39 (2010) 2120–2135.
[15] H. Li, J. Fan, X. Peng, Colourimetric and fluorescent probes for the optical detection of palladium ions, Chem. Soc. Rev. 42 (2013) 7943–7962.
[16] M.H. Lee, J.S. Kim, J.L. Sessler, Small molecule-based ratiometric fluorescence probes for cations, anions, and biomolecules, Chem. Soc. Rev. 44 (2015) 4185–4191.
[17] V.K. Gupta, A.K. Singh, L.K. Kumawat, Thiazole Schiff base turn-on fluorescent chemosensor for Al^{3+} ion, Sensors Actuators B Chem. 195 (2014) 98–108.
[18] V.K. Gupta, N. Mergu, L.K. Kumawat, A.K. Singh, A reversible fluorescence "off–on–off" sensor for sequential detection of aluminum and acetate/fluoride ions, Talanta 144 (2015) 80–89.
[19] V.K. Gupta, N. Mergu, L.K. Kumawat, A.K. Singh, Selective naked-eye detection of magnesium (II) ions using a coumarin-derived fluorescent probe, Sensors Actuators B Chem. 207 (2015) 216–223.
[20] V.K. Gupta, A.K. Jain, G. Maheshwari, Aluminum(III) selective potentiometric sensor based on morin in poly(vinyl chloride) matrix, Talanta 72 (2007) 1469–1473.
[21] V.K. Gupta, A.K. Jain, S. Agarwal, G. Maheshwari, An iron(III) ion-selective sensor based on a mu-bis(tridentate) ligand, Talanta 71 (2007) 1964–1968.
[22] V.K. Gupta, R.N. Goyal, R.A. Sharma, Anion recognition using newly synthesized hydrogen bonding disubstituted phenylhydrazone-based receptors: poly(vinyl chloride)-based sensor for acetate, Talanta 76 (2008) 859–864.
[23] R.N. Goyal, V.K. Gupta, S. Chatterjee, Voltammetric biosensors for the determination of paracetamol at carbon nanotube modified pyrolytic graphite electrode, Sensors Actuators B Chem. 149 (2010) 252–258.
[24] R.N. Goyal, V.K. Gupta, N. Bachheti, Fullerene-C-60-modified electrode as a sensitive voltammetric sensor for detection of nandrolone - an anabolic steroid used in doping, Anal. Chim. Acta 597 (2007) 82–89.
[25] K. Chen, Q. Shu, M. Schmittel, Design strategies for lab-on-a-molecule probes and orthogonal sensing, Chem. Soc. Rev. 44 (2015) 136–160.
[26] V.K. Gupta, S. Jain, U. Khurana, A PVC-based pentathia-15-crown-5 membrane potentiometric sensor for mercury(II), Electroanalysis 9 (1997) 478–480.
[27] V.K. Gupta, A.K. Singh, A. Al Khayat, B. Gupta, Neutral carriers based polymeric membrane electrodes for selective determination of mercury (II), Anal. Chim. Acta 590 (2007) 81–90.
[28] H. Khani, M.K. Rofouei, P. Arab, V.K. Gupta, Z. Vafaei, Multi-walled carbon nanotubes-ionic liquid-carbon paste electrode as a super selectivity sensor: application to potentiometric monitoring of mercury ion(II), J. Hazard. Mater. 183 (2010) 402–409.
[29] Z. Yang, J. Cao, Y. He, J.H. Yang, T. Kim, X. Peng, J.S. Kim, Macro−/micro-environment-sensitive chemosensing and biological imaging, Chem. Soc. Rev. 43 (2014) 4563–4601.
[30] R. Jain, V.K. Gupta, N. Jadon, K. Radhapyari, Voltammetric determination of cefixime in pharmaceuticals and biological fluids, Anal. Biochem. 407 (2010) 79–88.
[31] A.K. Jain, V.K. Gupta, L.P. Singh, J.R. Raisoni, A comparative study of Pb^{2+} selective sensors based on derivatized tetrapyrazole and calix 4 arene receptors, Electrochim. Acta 51 (2006) 2547–2553.
[32] V.K. Gupta, A.K. Singh, S. Mehtab, B. Gupta, A cobalt(II)-selective PVC membrane based on a Schiff base complex of N,N′-bis(salicylidene)-3,4-diaminotoluene, Anal. Chim. Acta 566 (2006) 5–10.
[33] M. Beija, C.A. Afonso, J.M. Martinho, Synthesis and applications of rhodamine derivatives as fluorescent probes, Chem. Soc. Rev. 38 (2009) 2410–2433.
[34] H.N. Kim, M.H. Lee, H.J. Kim, J.S. Kim, J. Yoon, A new trend in rhodamine-based chemosensors: application of spirolactam ring-opening to sensing ions, Chem. Soc. Rev. 37 (2008) 1465–1472.
[35] V. Dujols, F. Ford, A.W. Czarnik, A long-wavelength fluorescent chemodosimeter selective for Cu(II) ion in water, J. Am. Chem. Soc. 119 (1997) 7386–7387.
[36] Y. Xiang, A. Tong, P. Jin, Y. Ju, New fluorescent rhodamine hydrazone chemosensor for Cu(II) with high selectivity and sensitivity, Org. Lett. 8 (2006) 2863–2866.
[37] A. Bekhradnia, E. Domehri, M. Khosravi, Novel coumarin-based fluorescent probe for selective detection of Cu(II), Spectrochim. Acta A Mol. Biomol. Spectrosc. 152 (2016) 18–22.
[38] A. Ghorai, J. Mondal, S. Chowdhury, G.K. Patra, Solvent-dependent fluorescent-colorimetric probe for dual monitoring of Al^{3+} and Cu^{2+} in aqueous solution: an application to bio-imaging, Dalton Trans. 45 (2016) 11540–11553.
[39] K. Liu, H. Shang, F. Meng, Y. Liu, W. Lin, A novel near-infrared fluorescent platform with good photostability and the application for a reaction-based Cu^{2+} probe in living cells, Talanta 147 (2016) 193–198.
[40] H. Lu, H. Zhang, J. Chen, J. Zhang, R. Liu, H. Sun, Y. Zhao, Z. Chai, Y. Hu, A thiol fluorescent probe reveals the intricate modulation of cysteine's reactivity by Cu(II), Talanta 146 (2016) 477–482.
[41] M. She, Z. Yang, L. Hao, Z. Wang, T. Luo, M. Obst, P. Liu, Y. Shen, S. Zhang, J. Li, A novel approach to study the structure-property relationships and applications in living systems of Modular Cu^{2+} fluorescent probes, Sci. Report. 6 (2016).
[42] L. Tang, P. He, K. Zhong, S. Hou, Y. Bian, A new hydroxynaphthyl benzothiazole derived fluorescent probe for highly selective and sensitive Cu^{2+} detection, Spectrochim. Acta A Mol. Biomol. Spectrosc. 169 (2016) 246–251.
[43] J. Yang, L. Huang, Z. Guo, W. Ren, Q. Wang, A Cu(II)-benzoyl hydrazone based fluorescent probe for lipopolysaccharides, J. Lumin. 172 (2016) 290–296.
[44] V.K. Gupta, R. Prasad, A. Kumar, Cu(II) selective sensor based on 5,7,12,14-tetramethyldibenzo[b,i]-1,4,8,11-tetraazacyclotetradecane in PVC matrix, J. Appl. Electrochem. 33 (2003) 381–386.
[45] V.K. Gupta, B. Sethi, R.A. Sharma, S. Agarwal, A. Bharti, Mercury selective potentiometric sensor based on low rim functionalized thiacalix 4-arene as a cationic receptor, J. Mol. Liq. 177 (2013) 114–118.
[46] V.K. Gupta, M.L. Yola, N. Atar, Z. Ustundag, A.O. Solak, A novel sensitive Cu(II) and Cd(II) nanosensor platform: graphene oxide terminated p-aminophenyl modified glassy carbon surface, Electrochim. Acta 112 (2013) 541–548.
[47] V.K. Gupta, N. Mergu, L.K. Kumawat, A new multifunctional rhodamine-derived probe for colorimetric sensing of Cu(II) and Al(III) and fluorometric sensing of Fe(III) in aqueous media, Sensors Actuators B Chem. 223 (2016) 101–113.
[48] V.K. Gupta, L.P. Singh, R. Singh, N. Upadhyay, S.P. Kaur, B. Sethi, A novel copper (II) selective sensor based on dimethyl 4,4′(o-phenylene) bis(3-thioallophanate) in PVC matrix, J. Mol. Liq. 174 (2012) 11–16.
[49] H. Wynberg, E.W. Meijer, The Reimer–Tiemann reaction, Org. React. 28 (1982) 1.

[50] M.J. Frisch, G.W. Trucks, H.B. Schlegel, G.E. Scuseria, M.A. Robb, J.R. Cheeseman, G. Scalmani, V. Barone, B. Mennucci, G.A. Petersson, H. Nakatsuji, M. Caricato, X. Li, H.P. Hratchian, A.F. Izmaylov, J. Bloino, G. Zheng, J.L. Sonnenberg, M. Hada, M. Ehara, K. Toyota, R. Fukuda, J. Hasegawa, M. Ishida, T. Nakajima, Y. Honda, O. Kitao, H. Nakai, T. Vreven, J.A. Montgomery Jr., J.E. Peralta, F. Ogliaro, M. Bearpark, J.J. Heyd, E. Brothers, K.N. Kudin, V.N. Staroverov, R. Kobayashi, J. Normand, K. Raghavachari, A. Rendell, J.C. Burant, S.S. Iyengar, J. Tomasi, M. Cossi, N. Rega, J.M. Millam, M. Klene, J.E. Knox, J.B. Cross, V. Bakken, C. Adamo, J. Jaramillo, R. Gomperts, R.E. Stratmann, O. Yazyev, A.J. Austin, R. Cammi, C. Pomelli, J.W. Ochterski, R.L. Martin, K. Morokuma, V.G. Zakrzewski, G.A. Voth, P. Salvador, J.J. Dannenberg, S. Dapprich, A.D. Daniels, O. Farkas, J.B. Foresman, J.V. Ortiz, J. Cioslowski, D.J. Fox, Gaussian 09, Revision D.01, Gaussian Inc., Wallingford, CT, 2013.

[51] X. Ma, Z. Tan, G. Wei, D. Wei, Y. Du, Solvent controlled sugar-rhodamine fluorescence sensor for Cu^{2+} detection, Analyst 137 (2012) 1436–1439.

[52] W.-Y. Liu, H.-Y. Li, H.-S. Lv, B.-X. Zhao, J.-Y. Miao, A rhodamine chromene-based turn-on fluorescence probe for selectively imaging Cu^{2+} in living cell, Spectrochim. Acta A Mol. Biomol. Spectrosc. 95 (2012) 658–663.

[53] S. Goswami, D. Sen, A.K. Das, N.K. Das, K. Aich, H.-K. Fun, C.K. Quah, A.K. Maity, P. Saha, A new rhodamine-coumarin Cu^{2+} — selective colorimetric and 'off-on' fluorescence probe for effective use in chemistry and bioimaging along with its bound X-ray crystal structure, Sensors Actuators B Chem. 183 (2013) 518–525.

[54] S. Goswami, S. Maity, A.C. Maity, A.K. Maity, A.K. Das, P. Saha, A FRET-based rhodamine-benzimidazole conjugate as a Cu^{2+} — selective colorimetric and ratiometric fluorescence probe that functions as a cytoplasm marker, RSC Adv. 4 (2014) 6300–6305.

[55] J. Ding, L. Yuan, L. Gao, J. Chen, Fluorescence quenching of a rhodamine derivative: selectively sensing Cu^{2+} in acidic aqueous media, J. Lumin. 132 (2012) 1987–1993.